

Novel circularly polarized dielectric resonator antenna for microwave image sensing application

Original

Novel circularly polarized dielectric resonator antenna for microwave image sensing application / Singhwal, Sumer Singh; Kumar Kanaujia, Binod; Singh, Ajit; Kishor, Jugul. - In: MICROWAVE AND OPTICAL TECHNOLOGY LETTERS. - ISSN 0895-2477. - 61:7(2019), pp. 1821-1827. [10.1002/mop.31830]

Availability:

This version is available at: 11583/3003135 since: 2025-09-26T10:25:18Z

Publisher:

Wiley

Published

DOI:10.1002/mop.31830

Terms of use:

This article is made available under terms and conditions as specified in the corresponding bibliographic description in the repository

Publisher copyright

Wiley postprint/Author's Accepted Manuscript

This is the peer reviewed version of the above quoted article, which has been published in final form at <http://dx.doi.org/10.1002/mop.31830>. This article may be used for non-commercial purposes in accordance with Wiley Terms and Conditions for Use of Self-Archived Versions.

(Article begins on next page)

Novel Circularly Polarized Dielectric Resonator Antenna for Microwave Image Sensing Application

Sumer Singh Singhwal¹, Binod Kumar Kanaujia^{2*}, Ajit Singh³, Jugul Kishor⁴

¹Department of Electronics and Communication Engineering, Uttarakhand Technical University, Dehradun, India.

²School of Computational and Integrative Sciences, Jawaharlal Nehru University, New Delhi-110067, India

* Senior Member, IEEE

³BTK Institute of Technology, Dwarahat, Uttarakhand, India

⁴ Department of Electronics and Communication Engineering, National Institute of Technology, Delhi, India

Abstract- In this paper, a novel, simple and compact structure of dielectric resonator antenna is proposed, which provides wide bandwidth across proposed mm wave band for microwave image sensing with considerable gain using a lossy FR4 epoxy substrate and thick FR4 as DRA. A DR can be excited using four-line feed using a circular loop type feed network. These line feeds maintain phase difference of 90° to produce CP. This antenna provides approximate constant gain of 8.6dB on 25-26GHz band and 3dB axial ratio bandwidth is almost 1GHz from 25.2-26.2GHz. 10dB Impedance bandwidth is 24-27 GHz. This antenna can be used in microwave image sensing and wearable sensors applications, due to its compactness ($30 \times 30 \text{ mm}^2$), in mm wave band.

Index Terms—Microwave image sensing, rectangular DRA, circular polarisation, mm wave.

I. INTRODUCTION

IN today's time simplicity, ease of design and cost of antenna are paramount factors which should be backed by admirable performance, so that production cost of antenna is less and quality of reception using antenna is commendable. Antenna as a sensor have advantage of passive operation, low profile, small size, multiplexing capability compatibility with dielectric substrate etc. Antenna have flexibility of dual function of communication and sensing. So an antenna for sensing application required minimum number of components. These features discuss above make antenna sensor as a vital tool in sensing application. A scheme of antenna integration with electronics circuits such as processing, conditioning and biasing circuits are shown in [1,2]. Different types of antenna as a sensing element is demonstrated in [3]. They are used for the measurement of the various physical parameters. This chapter basically covers operational features and interrogation of battery less antenna sensor. Microwaves are now also used for a near field microwave image sensing in breast cancer detection [4]. With the advent of more compact antennas are increasing its application in microwave sensors is also observe in astronomy, remote sensing, medical imaging and wide array of scientific and medical application. At mm wave band many researchers proposed antenna for image sensing application by using different design methodology. In [5] C Jang-Soon Park et al., proposed tilted beam antenna at 28 GHz with beam scanning capability using waveguide WR28 for feeding antenna. In [6] Philip Ayiku Dzagbletey et al., proposed

stacked 1×7 microstrip linear antenna array at 28GHz for 5G using Taconic TLY-5 substrate with 14.7dBi gain at resonant frequency. In [7] Gerhard F. Hamberger et al., proposed Beamforming antenna array (1×10) having 15dBi gain and 1GHz impedance bandwidth using RO4350B substrate material. In [8] Chun-Xu Mao et al., reported 4×4 array for 5G communication using double substrate material which are RO 4003C and RO 5880. In [9] Osama Haraz et al., proposed patch antenna using EBG Ground Structure and Dielectric Superstrate at 28GHz using RT5880 substrate material. Researchers are motivated to find sensor applications in mm wave band so that in future 5G communications can be well equipped with microwave sensors. Wearable sensor is another challenge because it requires compact size and light weight sensors.

Dielectric Resonator are widely used in present times due to their advantages of low metallic losses, wide bandwidth, low dielectric losses, high gain and easy to achieve circular polarisation (CP) at higher modes. Circular polarisation antennas are always preferred over their linear polarized counterparts because of less multipath fading, ease of receiving of signals and less polarisation losses. In, [10] M. Chauhan et al., proposed cylindrical DRA for wireless sensor applications using Rogers RO3210 which gives 3.6dB gain at resonant frequency 6.7 GHz and peak gain of 6.8dB in operating band. Dash et al [11], proposed a triangular dielectric resonator antenna by using spiral fed for remote sensing application with gain 2.15dBi and 3.69dBi.

Rectangular DRA is easy to fabricate in comparison to cylindrical DRA which is widely discussed in literature because of different mathematical interpretation given by researchers [12-13]. Major theoretical study on DRA is on dielectric resonator having permittivity $\epsilon_r > 10$ because of various advantages of high permittivity resonator, such as good coupling, large storage of energy etc. In [14] Yong-Mei Pan et al, compared performances of low permittivity DRA ($\epsilon_r = 5$) with high permittivity DRA ($\epsilon_r = 10$) and authors concluded that a lower permittivity DRA is recommendable for increasing the bandwidth of the DRA but size of DRA is also increased then and mode excitation in low permittivity DRA is also tough.

Our proposed DRA structure consists of a conventional FR-4 substrate as a DR and a circular loop with four feeds. The circular ring microstrip line with four feeds is used to excite TE_{116} mode in the DR. Major achievements of this project are simple design (no slot or probe feed is used), small size and low cost. The proposed DRA is working in 24-27 GHz frequency band exhibit flat gain around 8.6 dBi and 3dB AR bandwidth of approximately 1 GHz. Figure 1 shows simulated and fabricated DRA. Antenna Design was simulated using HFSS software and mathematical equations are computed using MATLAB software.

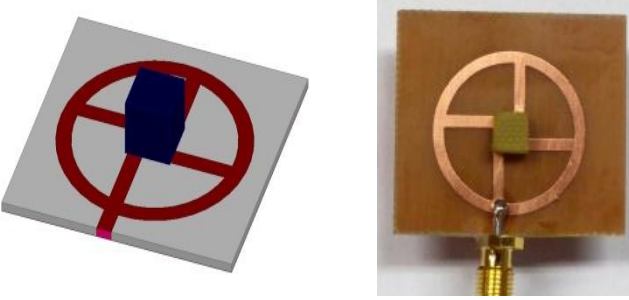
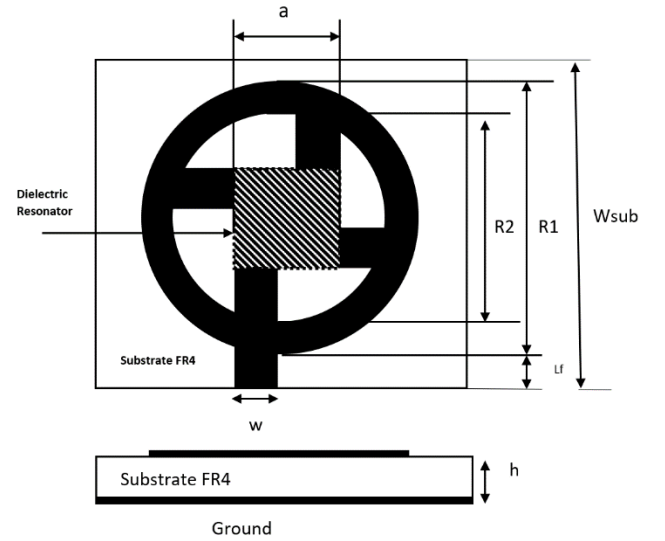
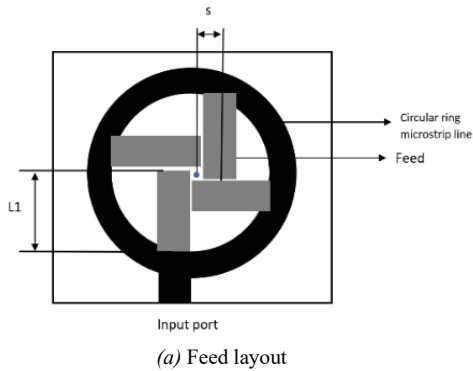


Figure 1 Simulated and fabricated antenna prototype



(b) Complete Layout with DRA

Figure 2. Layout of proposed design with parameters $w=1.93$ mm, $R1=12.29$ mm $R2=R1-w$, $h=0.8$ mm, $w_{sub} = 30$ mm, $Lr = 2.8$ mm, $s=1.645$ mm, $L1 = 10.5$ mm

II. DESIGN OF THE PROPOSED DRA

Figure 1 shows the layout of the proposed DRA antenna and its prototype. Figure 2 shows, the dimensional details of the proposed DRA. The proposed DRA consist of a circular loop with four feeds printed on a FR-4 substrate having $\epsilon_r=4.4$, $h=0.8$ mm, $\tan\delta=0.02$. An FR-4 substrate having dimension 5.85 mm \times 5.85 mm is utilized as a DR ($\epsilon_r=4.4$, $h_{dra}=4.8$ mm, $\tan\delta=0.02$) is placed on the DR such that it can cover four feed lines symmetrically. Width of circular ring microstrip line is calculated by using design equations given in [15].

A. Design of the DR

Mongia and Ittipiboon [16] studied DRA for dielectric constant ranging from 10-100. However, we have used the equation 1-4 [12,14] for the calculation of the dimension

$$k_x = \frac{\pi}{a} ; k_y = \frac{\pi}{b} \quad (1)$$

$$k_z \tan(k_z d/2) = \sqrt{(\epsilon_r - 1) k_0^2 - k_z^2} \quad (2)$$

$$k_x^2 + k_y^2 + k_z^2 = \epsilon_r k_0^2 \quad (3)$$

$$k_0 = \frac{2\pi f_0}{c} \quad (4)$$

Where k_x, k_y, k_z denotes wavenumbers along x, y, z directions respectively. k_0 denotes free space wavenumber

corresponding to resonant frequency f_0 .

By using MATLAB we obtain two values of the square DRA, which can satisfy equation 1-4, which are $5.62 \text{ mm} \times 5.62 \text{ mm} \times 1.6$ and $4.34 \text{ mm} \times 4.34 \text{ mm} \times 4.8 \text{ mm}$ respectively at frequency of interest. When designing a DRA by using these dimensions it did not resonated at the desired frequency. It was because of low dielectric constant DR material. So, the parametric analysis is performed to find out new dimension of the DRA which operated at desired frequency. After optimization, new dimension of the DRA is $5.85 \text{ mm} \times 5.85 \text{ mm} \times 4.8 \text{ mm}$ operation at 25.5 GHz which is chosen as middle value of targeted band 24-27GHz.

B. Operating Principle of the DRA

For the analysis of the proposed DRA, design and development of the DRA are divided in to two part, part one describes describe about feed network and part two explain about working of the DRA.

Part1: Figure 2 shows the proposed configuration of the feed networks. Design steps are shown in Figure 3. First step is shifted microstrip feed to excite DRA but it was unable to excite modes in DRA. In second step, four strips are used to excite modes in DRA which works good but isolation of all four feeds was very poor. In third step, a circular feed loop is added so that single feed can achieve the results. All the four strips are at equal distance on the circumference of the circular loop so that a 90° phase difference should be maintained between any two strips. So, when a signal applied to the feed, all four feeds experience current quadrature phase difference with each other.

Part2: A rectangular DRA placed centrally over the feed network. The DRA is coupled with four strip which have provided excitation of the rectangular DRA, which led the rectangular DRA to resonate at 25.6 GHz. interestingly, this circular loop setup provides excitation to the rectangular DRA with 90° phase difference hence provide circular polarization.

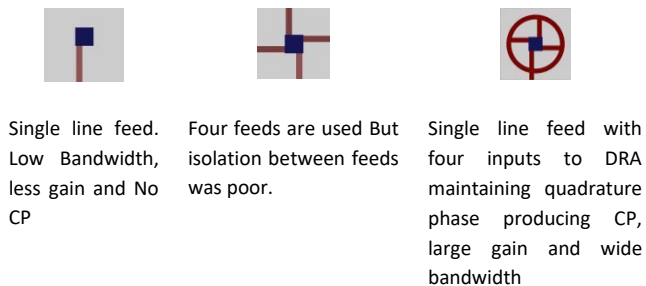


Figure 3. Design steps of Antenna

The excitation of different mode in rectangular DRA depends upon feed mechanism. Here, the rectangular DRA is excited

by using four strips. Rectangular DRA produce pure modes when excited in isolated condition but grounded DRA with four sequential feeds with single main feed, excites DRA asymmetrically, which gave $TE_{11\delta}$ mode which is confirmed by magnetic field distribution, as shown in Figure 4 (a, b), as explained in [17]. It is also confirmed from Figure 4(c), which were defined by [16] for $TE_{11\delta}$.

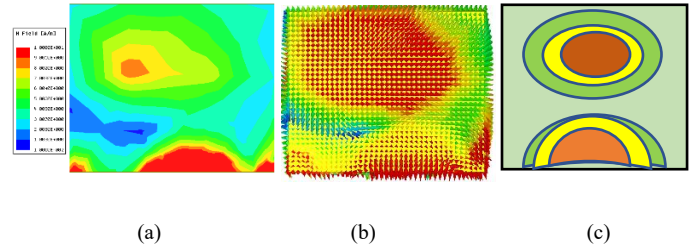


Figure 4. Magnetic Field distribution on DRA on y-z plane at 25.6 GHz (a) Magnitude (b) Vector (c) Theoretical

It was worth mentioning that radius of circular loop also participate in performance of DRA. We optimized the circular loop radius for best impedance matching, wide axial ratio (AR) bandwidth and commendable gain throughout band.

III. PARAMETRIC ANALYSIS

Various dimensions have been analyzed to get broad impedance bandwidth with good stable gain. To understand behavior of design parameters, a parametric analysis is studied. It was studied while doing analysis that radius of circular loop (R_1) and height of DRA (h_{dra}) affects the results of proposed antenna in terms of gain and bandwidth.

A. Effect of radius of loop

First parametric analysis was implemented for studying effect of radius of loop. Parameters observed are reflection coefficient, gain and axial ratio which are shown in figure 5-7.

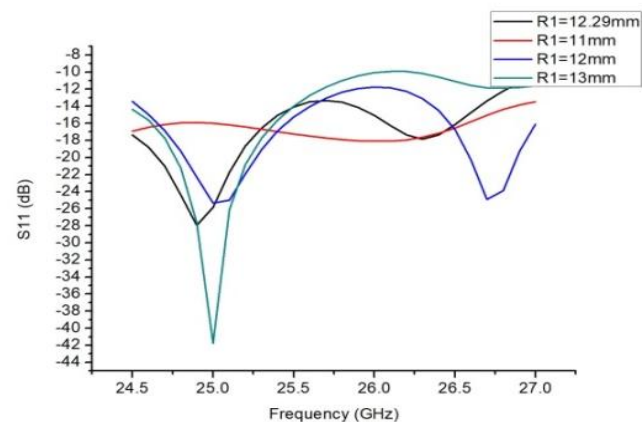


Figure 5: Reflection coefficient (dB) vs. frequency (GHz) for parametric variation of loop radius with fixed height of DRA of 4.8 mm

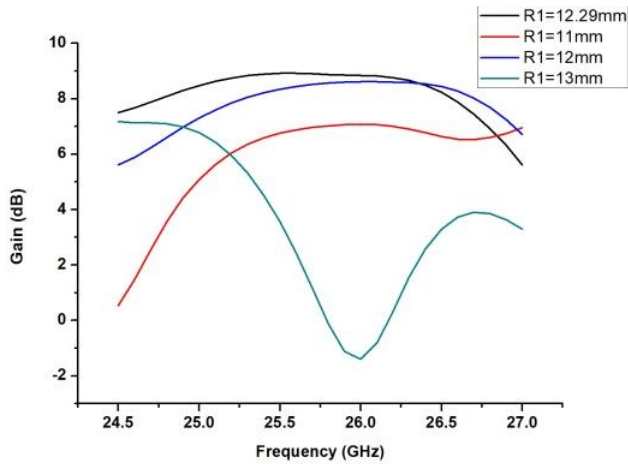
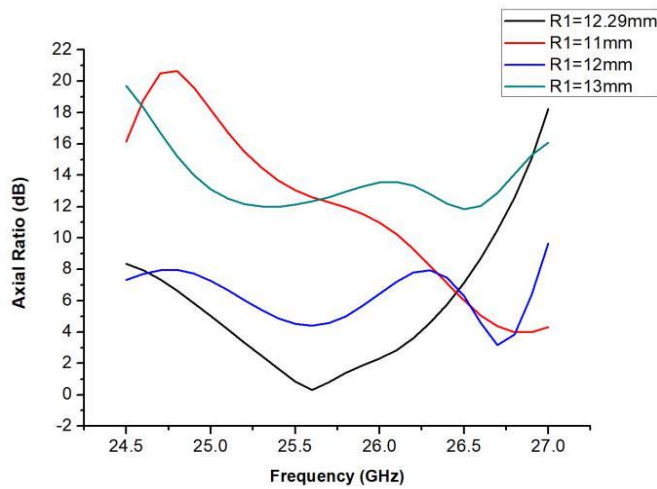


Figure 6: Gain (dB) vs. frequency (GHz) for parametric



variation of loop radius with fixed height of DRA of 4.8 mm

Figure 7: Axial Ratio (dB) vs. frequency (GHz) for parametric variation of loop radius with fixed height of DRA of 4.8 mm

It was observed that reflection coefficient is achieved less than -10dB for all variation of loop radius and gain also varies with respect to loop radius. Gain is maximum for loop radius of 12.29mm. Table-1 summarizes all the finding of parametric analysis for effect of loop radius. It is clearly visible from table 1 that AR bandwidth is achieved only for the case of radius 12.29mm and also flat gain around 8.6dB is achieved for this optimized radius of loop.

Table 1 : Summary of Parametric effects of loop radius

| Radius of Loop (mm) | Impedance Bandwidth (GHz) | Resonant Frequency (GHz) | Reflection Coefficient (dB) | Peak Gain (dB) | AR Bandwidth (GHz) |
|---------------------|---------------------------|--------------------------|-----------------------------|--------------------|--------------------|
| 11 | 24-27 | 25 | -16 | 6.2 | - |
| 12 | 24-27 | 25 | -25 | 8.2 (Flat Gain) | - |
| 12.29 | 24-27 | 24.9 | -28 | 8.6 (Flat Gain) | 25.2-26.2 |
| 13 | 24-26 | 25 | -42 | 6.8 | - |

B. Effect of height of DRA

Second parametric analysis is studied for height of DRA which is taken multiple of 1.6mm as it is easily available commercially. Variation of standard parameters like reflection coefficient, gain and axial ratio with respect to change in height of DRA is shown in figure 8-10.

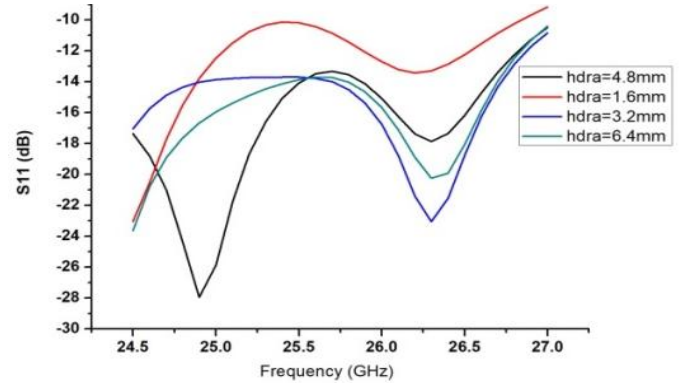


Figure 8: Reflection coefficient (dB) vs. frequency (GHz) for parametric variation of height of DRA with loop radius of 12.29mm

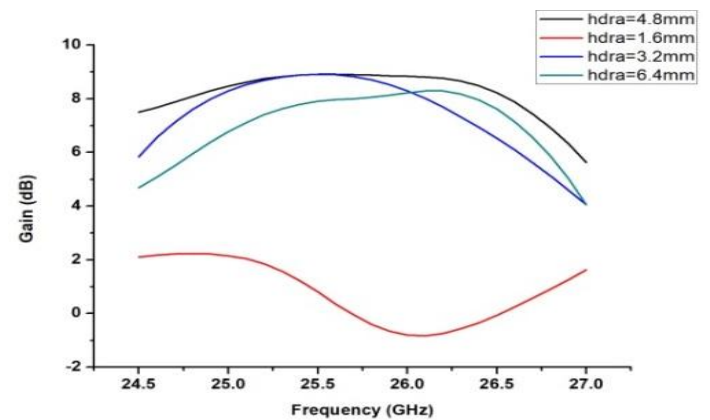


Figure 9: Gain (dB) vs. frequency (GHz) for parametric variation of height of DRA with fixed loop radius of 12.29mm

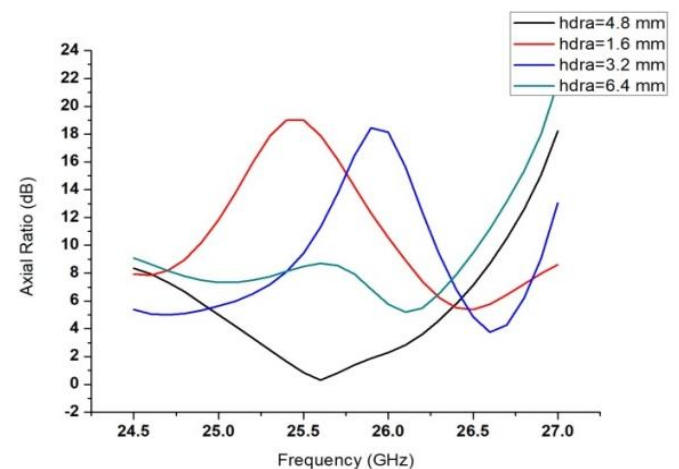


Figure 10: Axial Ratio (dB) vs. frequency (GHz) for parametric variation of height of DRA with fixed loop radius of 12.29mm

It was analyzed from figure 8-10 that reflection coefficient achieved at 24.9GHz frequency is -28dB for height of DRA 4.8mm and as we increase or decrease height reflection coefficient at resonant frequency increases. Major observation is that gain becomes stable for 4.8mm height for 24.5-26.5 GHz band. Next performance parameter which confirms our proposed height is axial ratio bandwidth. Axial ratio bandwidth of approximately 1GHz is achieved centered around resonant frequency 25.6GHz for 4.8mm height. Table-2 summarizes all the findings of parametric study of effect of height of DRA.

Table 2 : Summary of parametric effects of height of DRA

| Height of DRA (mm) | Impedance Bandwidth (GHz) | Resonant Frequency (GHz) | Reflection Coefficient (dB) | Peak Gain (dB) | AR Bandwidth (GHz) |
|--------------------|---------------------------|--------------------------|-----------------------------|------------------------|--------------------|
| 1.6 | 24-27 | 26.3 | -12 | 2 | - |
| 3.2 | 24-27 | 26.3 | -18 | 8.55 | - |
| 4.8 | 24-27 | 24.9 | -28 | 8.6 (Flat Gain) | 25.2-26.2 |
| 6.4 | 24-27 | 26.2 | -22 | 7.6 | - |

It can be concluded from both parametric analysis that our choice of taking height of DRA and radius of loop is justified to achieve circular polarisation, wide impedance bandwidth and high stable gain all over the band of interest.

IV. RESULTS AND DISCUSSION

In this section, validation of proposed rectangular DRA is discussed. A prototype antenna based on the FR-4 DR is fabricated, which is shown in the Fig. 1. Agilent N5230A vector network analyzer is used to measure impedance bandwidth of the fabricated antenna. Figure 6(a) shows, the simulated and measured $|S_{11}|$ of the rectangular DRA. It can be observed that measured and simulated impedance bandwidth cover the 24-27 GHz frequency band. Similarly, 3dB AR Bandwidth of 1 GHz (25.2 GHz to 26.2 GHz) is achieved, as shown in the Fig. 12. A close agreement can be observed between 3-dB axial ratio bandwidth of measured and simulated plots. The measured and simulated radiation pattern in broadside direction is plotted in the figure 13. From the radiation pattern half power beamwidth of 70° and Front to Back ratio of 16.9 dB is calculated. Figure-14 shows co-polarisation and cross polarisation graph which shows good separation of 20dB between co-pol and x-pol component in H-plane ($\phi=90^\circ$) at resonance frequency 25.6GHz. Our prototype agrees with measured results with some deviation due to fabrication constraints at noncommercial level.

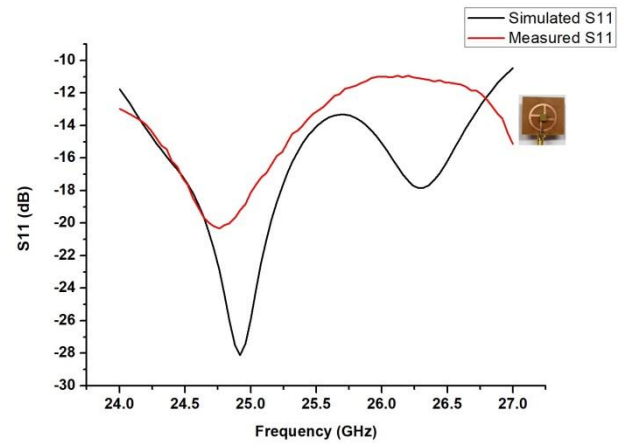


Figure 11: Reflection coefficient (db) vs frequency (GHz) comparison between simulated and measured results

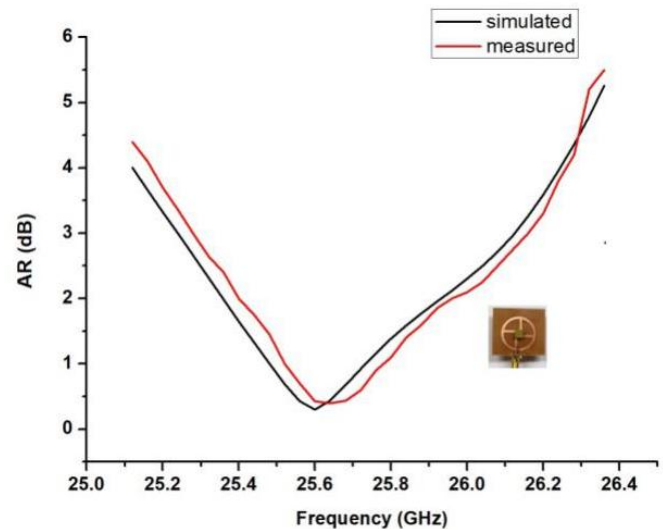


Figure 12: Axial ratio (dB) vs. frequency (GHz) comparison between simulated and measured results

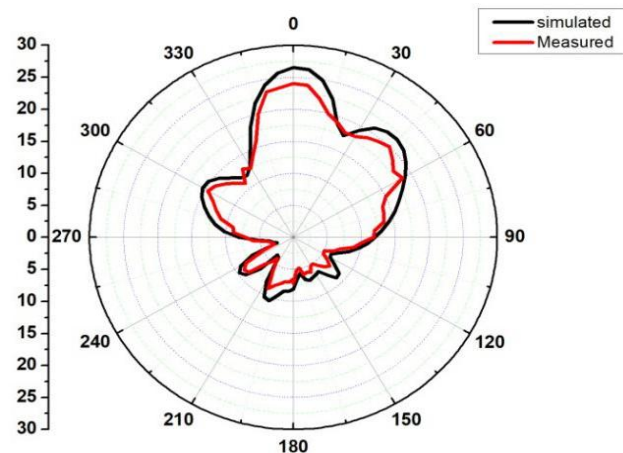


Figure 13: Comparison of radiation pattern of simulated and measured antenna

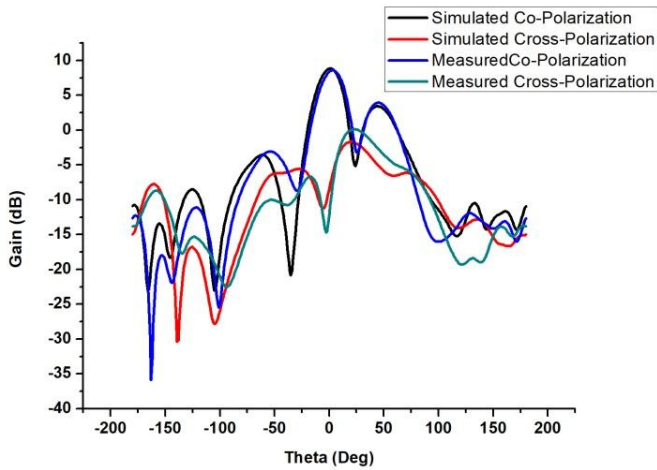


Figure 14: Gain (Co-polarisation) dB vs. frequency (GHz) and Gain (Cross-Polarisation) dB vs. frequency (GHz) comparison between simulated and measured results

Our proposed DRA also supports linear polarisation in UWB from 22.5-27GHz with peak gain of 8.6dB. Figure 15 demonstrates linear polarisation and circular polarisation bandwidth. It shows gain and reflection coefficient variation with respect to frequency. Area covered by red rectangle with bandwidth 25.2-26.2GHz covers circular polarisation with high gain but remaining band from 22.5-27 GHz have variable gain and may be used for broad bandwidth applications. When transmitters and receivers are static or fixed then linear polarisation is also preferred depending upon the application. In microwave sensing application often sensors may be fixed at certain position such as in satellites, mobile communication.

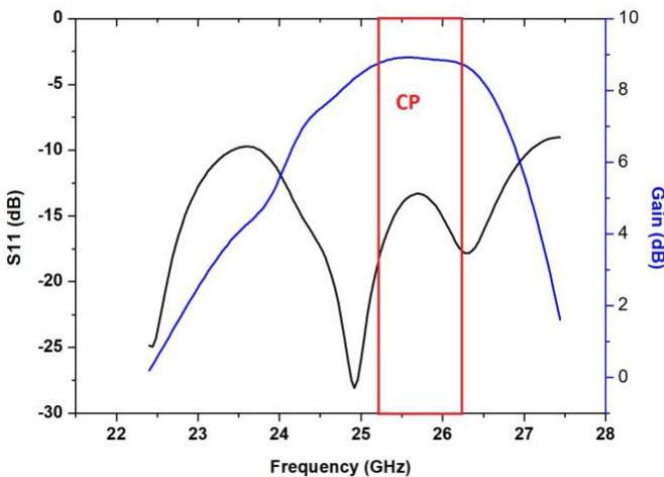


Figure 15: Gain (dB), Reflection Coefficient (dB) versus frequency (GHz) plot

V. CONCLUSION

Presently only high permittivity DR are used due their multiple advantages. In microwave image sensing, cost is an important factor to consider because a sensor is always followed by signal processing circuitry, so overall cost of the system will be increased. For the microwave image sensing application, the gain of the device should be high and stable.

The proposed DRA fulfill all the basic condition of the sensor. Proposed DRA can offer wide impedance bandwidth and AR bandwidth which is also desirable feather of the sensor.

So, to reduce overall cost of system and improve performance, proposed prototype can be a good choice for image sensing applications at mm wave band such as satellite communication applications, 5G communications [18] etc. CEPT documentation available on [19] concludes that 24.5-27.5GHz band is good candidate for 5G communication and harmonization is possible on this band all over the globe. According to [20], 28GHz band is proposed for ESIM (Earth Stations in Motion) remote sensing and IMT (International Mobile Telecommunications) standards which are relevant to microwave remote sensing. Our proposed antenna covers this band and can be used as an image sensor in IMT standards and ESIM remote sensing applications. It is very small size comparable to wrist watch dial and DRA height 0.48cm, so it can also be used in wearable body sensors in mm wave band. Due to its low cost commercial scalability is also possible.

REFERENCES

- [1] Cándid Reig, Ernesto Ávila-Navarro. "Printed Antennas for Sensor Applications: A Review," IEEE Sensors Journal, Vol. 134, No. 8, 2013
- [2] Huang H. "Flexible Wireless Antenna Sensor: A Review," IEEE Sensors Journal, Vol. 13 , No. 10, 2013
- [3] Huang H. "Antenna Sensors in Passive Wireless Sensing Systems," In: Chen Z. (eds) Handbook of Antenna Technologies. Springer, Singapore, 2015.
- [4] A. Mirza et al, "An Active Microwave Sensor for Near Field Imaging", IEEE Sensors Journal (Volume: 17, Issue: 9, May1, 1 2017)
- [5] C Jang-Soon Park et al. "A tilted combined beam antenna for 5G communications using a 28 GHz band", IEEE Antennas and Wireless Propagation Letters. DOI 10.1109/LAWP.2016.2523514
- [6] Philip Ayiku Dzagbletey et al., "Stacked microstrip linear array with highly suppressed side-lobe levels and wide bandwidth", IET Microwaves, Antennas & Propagation, June 2016 DOI: 10.1049/iet-map.2016.0161.
- [7] Gerhard F. Hamberger et al. , "A Planar Dual-Polarized Microstrip 1D-Beamforming Antenna Array for the 24 GHz Band", IEEE Transactions on Antennas and Propagation, 2016 DOI 10.1109/TAP.2016.2618847 .
- [8] Chun-Xu Mao et al., "Broadband High-Gain Beam-Scanning Antenna Array for Millimeter-Wave Applications", IEEE Transactions on Antennas and Propagation, 2017. DOI 10.1109/TAP.2017.2724640
- [9] Osama Haraz et al., "Dense Dielectric Patch Array Antenna With Improved Radiation Characteristics Using EBG Ground Structure and Dielectric Superstrate for Future 5G Cellular Networks" IEEE Access Volume-2, 2014. DOI. 10.1109/ACCESS.2014.2352679
- [10] M. Chauhan et al., "A novel Compact Cylindrical Dielectric Resonator Antenna for Wireless Sensor Network application", IEEE Sensors Letters, 2016. DOI 10.1109/LSSENS.2018.2825369
- [11] S.K. Dash et al, "Circularly Polarized Dual Facet Spiral Fed Compact Triangular Dielectric Resonator Antenna for Sensing Applications", IEEE Sensors Letters Volume-2(3), 2017.
- [12] A. Petosa, *Dielectric Resonator Antenna Handbook*, Artech Publication House, 2007
- [13] K. M. Luk and K. W. Leung, Eds., *Dielectric Resonator Antennas*. Baldock, U.K.: Research Studies Press, 2003.
- [14] Yong-Mei Pan et al, "Design of the Millimeter-wave Rectangular Dielectric Resonator Antenna Using a Higher-Order Mode", IEEE Transactions on Antennas and Propagation, Vol. 59, No. 8, August 2011.
- [15] K.C.Gupta., R.Garg, P.Bhartia and I.Bahl, "Microstrip Lines and Slotlines " Artech House, 1996
- [16] R.K. Mongia and A. Ittipiboon, "Theoretical and Experimental Investigations on Rectangular Dielectric Resonator Antennas", IEEE

Transactions on Antennas and Propagation, Vol. 45, No. 9, September 1997.

- [17] R.S. Yaduvanshi and H Parthasarathy, “*Rectangular Dielectric Resonator Antennas Theory and Design*” published by Springer. ISBN 978-81-322-2500-3 (eBook)
- [18] Debatosh Guha and Chandrakanta Kumar, "Microstrip Patch versus Dielectric Resonator Antenna Bearing All Commonly Used Feeds", IEEE Antennas & Propagation Magazine, Feb 2016
- [19] 5G and IMT identification-CEPT online available at <https://www.itu.int/en/ITU-R/seminars/rrs/2017-Africa/Forum/CEPT-ECC.pdf>.
- [20] Paolo de Mattheis et al. “Spectrum Management and Its Importance for Microwave Remote Sensing” , IEEE Geoscience and Remote Sensing Magazine, June 2018.